4-21-2012

A Plant Virus Substrate Induces Early Upregulation of BMP2 for Rapid Bone Formation

Pongkwan Sitasuwan
University of South Carolina - Columbia

L. Andrew Lee
University of South Carolina - Columbia

Peng Bo
Chinese Academy of Sciences

Erin N. Davis
University of South Carolina - Columbia

Yuan Lin
University of South Carolina - Columbia, wang@mail.chem.sc.edu

See next page for additional authors

Publication Info

Published in *Integrative Biology*, Volume 4, Issue 6, 2012, pages 651-660.

Integrative Biology

Cite this: *Integr. Biol.*, 2012, **4**, 651–660

www.rsc.org/ibiology

PAPER

A plant virus substrate induces early upregulation of BMP2 for rapid bone formation†

Pongkwan Sitasuwan,[a] L. Andrew Lee,[a] Peng Bo,[b] Erin N. Davis,[a] Yuan Lin*[b] and Qian Wang*[a]

Received 24th February 2012, Accepted 21st March 2012
DOI: 10.1039/c2ib20041d

Many nanoscale materials have been developed to investigate the effects on stem cell differentiations *via* topographical and chemical cues for applications in tissue engineering and regenerative medicine. The use of plant viruses as cell supporting substrates has been of particular interest due to the rapid induction of bone marrow derived mesenchymal stem cells (BMSCs) towards osteogenic cells. In this study, the role of *Tobacco mosaic virus* (TMV) and its early effects on osteoinduction with particular emphasis on the regulation of bone morphogenetic protein-2 (BMP2) was examined. We observed that the cells on the virus substrate immediately aggregated and formed bone-like nodules within 24 hours. An immediate increase in BMP2 gene and protein expression for cells on the TMV substrate was observed within 8 hours of osteoinduction. Moreover, BMP2 expression was highly localized to cells within the cell aggregates. This enhanced differentiation only occurred when TMV was coated on a solid support but not upon adding the virus to the media solution. Taken together, the results from this study highlight the potential of virus-based nanomaterials to promote endogenous BMP2 production which may prove to be a unique approach to studying the regulatory mechanisms involved in early osteoblastic differentiation.

Introduction

Stem cell fate is dependent on the surrounding stimuli, including both soluble and insoluble factors. How stem cells respond to different nanoscale cues has been extensively studied for tissue engineering and regenerative medicine applications.[1] There are several reports indicating that stem cell differentiation can be dictated at the nanometre level.[2,3] Bone marrow derived mesenchymal stem cells (BMSCs) are from the non-hematopoietic sub-population of bone marrow stroma,[4,5] which have the ability to self-renew and differentiate to various lineages, such as adipocytes, osteocytes, chondrocytes, hepatocytes, neurons, muscle cells, and epithelial cells.[5,6] The pluripotent potential of BMSCs, ease of isolation, rapid expansion,[7] and less controversial use than embryonic stem cells make this cell type an ideal source of adult stem cells to study material-mediated differentiation.

Recently, we have reported accelerated osteogenic differentiation of BMSCs grown on plant virus coated substrates in comparison to cells cultured on conventional tissue culture plastic (TCP).[8,9] Two different plant viruses were employed in those studies, *i.e.* spherical *Turnip yellow mosaic virus* (TYMV)

[a] *Department of Chemistry and Biochemistry, University of South Carolina, 631 Sumter Street, Columbia, SC 29208, USA. E-mail: wang@mail.chem.sc.edu; Fax: +1 803 777 9521; Tel: +1 803 777 8436*
[b] *State Key Laboratory of Polymer Physics and Chemistry, Changchun Institute of Applied Chemistry, Chinese Academy of Sciences, Changchun 130022, PR China. E-mail: linyuan@ciac.jl.cn*
† Electronic supplementary information (ESI) available. See DOI: 10.1039/c2ib20041d

Insight, innovation, integration

Bone morphogenetic protein-2 (BMP2) is a potent growth factor that is supplemented to induce bone differentiation in many conventional tissue differentiation studies. Here, we report that by using plant virus as a biocompatible nanomaterial, endogenous expression of BMP2 can be induced in mesenchymal stem cells to direct differentiation towards osteoblasts. This enhanced differentiation only occurs when virus is coated on a solid support but not with the addition of virus as a solution to the media. Therefore, the possibility of such nanomaterials that increase endogenous BMP2 production is highly relevant for BMP2 mediated stem cell differentiation and future bone replacement therapies.

and rod-like *Tobacco mosaic virus* (TMV). In both situations, several key mRNA markers associated with bone differentiation peaked at day 14 for cells on virus-coated substrates, whereas the cells on conventional plates required additional 7 days to reach similar expression profiles.[8,9] Moreover, immunohistochemical staining for osteoblastic specific differentiation markers, osteocalcin, osteonectin, and osteopontin, had supported the gene expression profiles on day 14. The expressions of such osteogenic markers were further enhanced upon chemically modifying the virus with phosphates as indicated by increased Ca^{2+} mineralization and even higher mRNA expression levels of osteocalcin.[10] More importantly, gene profile studies of total mRNA and real time PCR suggested an early upregulation of endogenous mRNA levels of bone morphogenetic protein-2 (BMP2). This increase in the BMP2 mRNA level was observed for BMSCs cultured on TMV substrates within 24 hours of osteoinduction, which we speculate may be a key factor in the enhanced differentiation of BMSCs on virus coated substrates.[8]

BMP2 is a member of the bone morphogenetic protein subgroup within the transforming growth factor β (TGF-β) super family. Among the bone morphogenetic proteins (BMPs), the role of BMP2 in osteoblast differentiation and bone formation during embryonic skeletal development and postnatal bone remodelling has been extensively investigated.[11] Animal studies have shown that *BMP2* mRNA expression was at the maximal level within 24 hours of murine fracture injury, indicating that BMP2 is highly involved in bone repair initiation.[12] The results from another study showed that BMP2, BMP6, and BMP9 were potent inducers of mesenchymal stem cell differentiation towards osteoblasts.[13] Recombinant human BMP2 (rhBMP2) is commercially available and used as a therapeutic supplement for bone repair in spine fusion surgeries and tibial fracture healing.[14] The supplement can promote faster bone fusion for patients with back pain by promoting bone formation *in vivo*, and many hydrogel encapsulation studies have shown enhanced osteogenic differentiation of MSCs *in vitro*.[15] However, rhBMP2 is costly and some recent studies reported the adverse effects caused by implant failure or leakage causing life-threatening urogenital events, retrograde ejaculation, back and leg pain, hematoma, or breathing difficulty.[16] Therefore, the use of nanoscale materials to promote endogenous BMP2 production becomes an extremely attractive route for studying the mechanisms involved in bone tissue repair. This report is to examine the virus-based system and its role in early differentiation of BMSCs by monitoring its ability to upregulate BMP2 expression.

TMV is a rod-shaped particle measuring 300 nm in length with a diameter of 18 nm. The shape of the plant virus resembles the size scales of fibrillar extracellular matrix (ECM) protein, such as collagen. The viral capsid consists of 2130 identical coat protein subunits assembled in a helical structure around the single stranded genomic RNA. The production of TMV is cost effective and the resulting viral particles are highly uniform in size. The ability of TMV to be easily and uniformly manipulated *via* chemical[10,17] and genetic modifications[18] has gained traction as novel biomaterials for potential tissue engineering applications.[19,20] Herein, we report the early molecular events that occur within the first 24 hours of osteoinduction in BMSCs when cultured on TMV-coated substrates. The results indicate that BMP2 mRNA expression is dramatically increased within 8 hours of osteoinduction and protein expression was found to be highly localized to the cell clumps. The virus coating provided a significant increase in BMP2 mRNA levels in comparison to dexamethasone treatment alone. However, the addition of dexamethasone in the presence of the virus provided the greatest enhancement in BMP2 gene expression. The results from QCM-D and TMV supplemented cultures suggest that dexamethasone and TMV act independently on BMP2 expression. Extended analyses with cytokine arrays showed that different cytokines were present in the conditioned media from cells cultured on TMV-coated substrates; however, these cytokines have not previously been associated with early osteogenic differentiation. Alternatively, actin polymerization appeared to be congruent with the recent report associating actin depolymerisation and mineralization.[25] The results reported in this study clearly support the role of TMV coated substrates acting synergistically with dexamethasone to regulate early BMP2 expression and ultimately enhance stem cell differentiation.

Results and discussion

The morphological differences of BMSCs on TCP *versus* TMV substrates

The morphological differences of BMSCs cultured on TCP or TMV coated substrates (*e.g.* 3-aminopropyltriethoxysilane (APTES) grafted coverslips) were imaged at the early time points. After 6 hours in basal media, cells on TCP fully spread on the substrate (Fig. 1A), whereas cells seeded on TMV wafers partially spread (Fig. 1D). 24 Hours after seeding, BMSCs on the TCP sample continued to spread and cover the entire substrate (Fig. 1B), whereas the cells on TMV-coated substrates aggregated to form nodule-like cell clumps (Fig. 1E). After 24 hours of culture in basal media, the media were changed to osteogenic media and the cells were imaged again 8 hours later. The cells on TCP remained spread out with no aggregation (Fig. 1C), and the cells on TMV substrates continued to form larger aggregates (Fig. 1F).

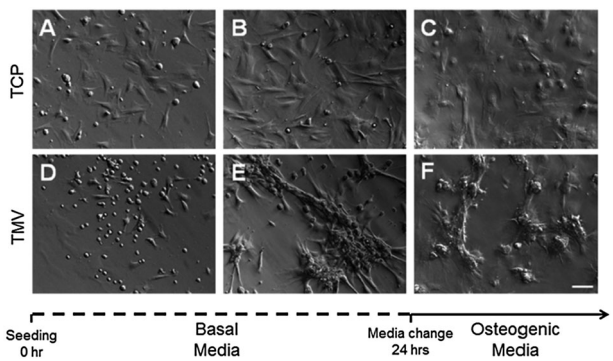

Fig. 1 Differential interference contrast (DIC) images of BMSCs on TCP and TMV substrates showing morphological changes over culture time. The time points are (A, D) 6 hours and (B, E) 24 hours after seeding in basal media, followed by (C, F) 8 hours in osteogenic media. The cells on standard TCP are well spread (A–C), whereas the cells on TMV coated substrates are often rounded and poorly spread (D–F). Scale bar is 100 μm.

Cell adhesion and spreading are highly dependent on the substrate surface. Interestingly, in this study, the cell morphologies were distinct as early as at 6 hour post seeding. The difference in cell shapes observed indicates altered cellular responses. Gene and protein analyses during the first 24 hours of osteoinduction were carried out to identify how TMV substrates could enhance osteogenesis of BMSCs. In order to examine if TMV is capable of chemically inducing the changes, the supplement of TMV into culture media was included in all studies. It is important to note that the morphology of BMSCs grown in media supplemented with TMV remained the same as that of TCP control (*data not shown*).

TMV on the surface alters *BMP2* and *IBSP* gene expression

In the previous study, we found enhanced osteogenic differentiation of BMSCs when cultured on TMV coated APTES glass coverslips.[8] Without TMV coating, the APTES glass coverslips showed similar effects to uncoated glass and TCP.[9] Microarray analysis of total cellular mRNA and real time PCR results indicated that the BMP2 mRNA level was higher in cells cultured on TMV coated substrates than in cells on TCP.[8] Based on these results, we examined the temporal changes in gene expression involved in early differentiation (*ALPL*, *BMP2* and *IBSP*) of cells cultured on TMV coated substrates, cells supplemented with TMV in solution, and cells cultured on conventional TCP (Fig. 2). Although there was no significant difference in the alkaline phosphatase gene *(ALPL)* mRNA expression for cells cultured on the three different substrates after 8 hours, the expression significantly increased after 24 hours in cells cultured on TMV substrates (Fig. 2A). However, the increase only exhibits less than two-fold difference over uninduced cells. Since alkaline phosphatase (ALP) is an enzyme that facilitates matrix mineralization and gradually increases over a period of 2 weeks,[21] it is possible that the time point of this study is too early to observe any significant upregulation in *ALPL* mRNA expression.

For cells cultured on TMV coated substrates, *BMP2* expression levels were six-fold higher than uninduced cultures after 8 hours of osteoinduction. In comparison, the cells in traditional cultures had only slightly increased *BMP2* gene expression by two-fold (Fig. 2B). The initial increase in *BMP2* gene expression for TCP had diminished back to the basal level after 24 hours, whereas the cells cultured on TMV coated substrates still maintained higher *BMP2* gene expression levels, a three-fold increase over TCP substrates (Fig. 2B). Although the addition of TMV as a solution supplement to the culture media resulted in a modest increase in *BMP2* expression at 24 hours, it failed to provide the same effects as the virus-coated substrates. The initial results with TMV in solution indicate that the coating of the virus to the solid support is necessary to affect early *BMP2* gene expression and the virus itself does not act as a soluble inducer. The results also suggest that TMV coated substrates enhance osteogenic differentiation of BMSCs by increasing *BMP2* mRNA levels.

In addition to increased *BMP2* gene expression, mRNA levels for integrin-binding sialoprotein (*IBSP*), a secreted extracellular matrix protein required for hydroxyapatite formation, increased over time in both TCP and TMV samples.

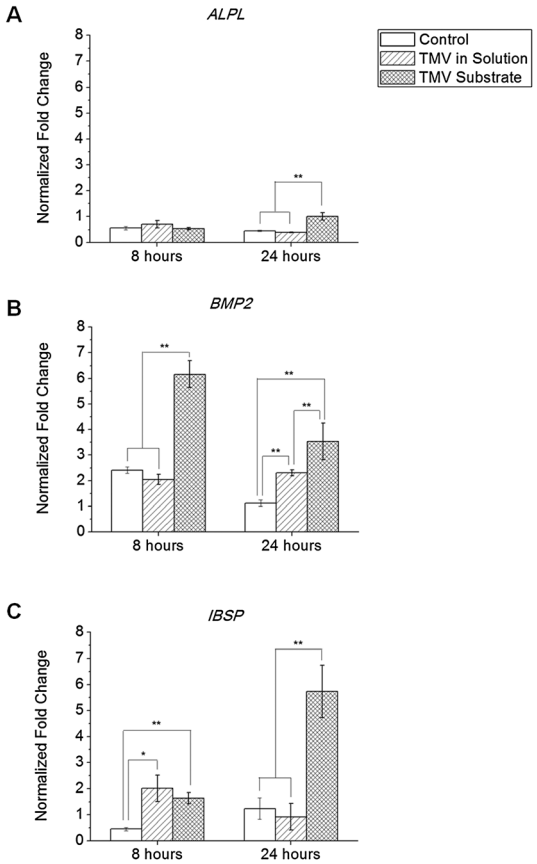

Fig. 2 RT-qPCR analysis of osteospecific gene expression of BMSCs under osteogenic conditions. For each growing condition, the profiles showed two time points: 8 and 24 hours after induction with osteogenic media. Gene expression in the cells seeded on TCP, TCP with TMV in solution and TMV substrates under osteogenic conditions. (A) *ALPL* expression was upregulated in cells grown on TMV at 24 hours. (B) *BMP2* expression at both time points was significantly increased in cells grown on TMV substrates. (C) *IBSP* was highly expressed in cells grown on TMV substrates at both time points. In all graphs, the error bars denote ±1 s.d. ** and * represent $p < 0.05$ and $p < 0.1$, respectively.

IBSP is an osteogenic marker associated with mineralizing tissues,[22] hence the increase in *IBSP* gene expression within 24 hours is an important discovery in explaining the role of TMV in osteogenic differentiation.[8] *IBSP* gene expression levels for cells grown on TMV were two-fold higher than those on TCP after 8 hours of osteoinduction and the difference further increased to five-fold after 24 hours (Fig. 2C). The addition of TMV as a solution to the culture media did not provide a similar increase in *IBSP* expression levels to TMV coated substrates (Fig. 2C).

The apparent increase in *BMP2* and *IBSP* mRNA levels for the cells on TMV-coated substrates suggests that these two proteins are involved in the enhancement of osteogenic differentiation (Fig. 2B and C). The observed differences in gene expression of *BMP2* and *IBSP* indicate that the surface coating with the virus moderates *BMP2* and *IBSP* expression levels within the first day, and the virus itself does not act as a soluble chemical inducer, but rather as a substrate with unique topographical features, or offer a rough surface, at both nanometre

and micrometre scales. Such surface features have been observed with M13 bacteriophage and TMV to affect cell directionality and ECM protein deposition.[20,23] It was demonstrated that nanoscale topography (*e.g.* roughness) directly influences cell adhesion leading to altered cellular behaviours including proliferation and differentiation.[3,24] The topographical features of TMV substrates before and after incubation in media observed by atomic force microscopy revealed such rough surfaces from the TMV coating, which was still visible after 24 hours of cell culture (Fig. S1, ESI†).

TMV substrate induces higher localized BMP2 production

The increase in the *BMP2* mRNA expression level was corroborated by ELISA, showing a similar trend to BMP2 increase at 8 and 24 hours in osteogenic media (Fig. 3A). In comparison to uninduced controls, the cells on TMV coated substrates expressed four-fold and three-fold higher levels of BMP2 at 8 and 24 hours, respectively. For TCP culture, there was no significant increase in BMP2 production at either time point (Fig. 3A). Although the addition of TMV in solution showed an increase in the *BMP2* mRNA level after 24 hours (Fig. 2B), the protein analysis did not validate this temporal increase (Fig. 3A). Thus, among the three growth conditions,

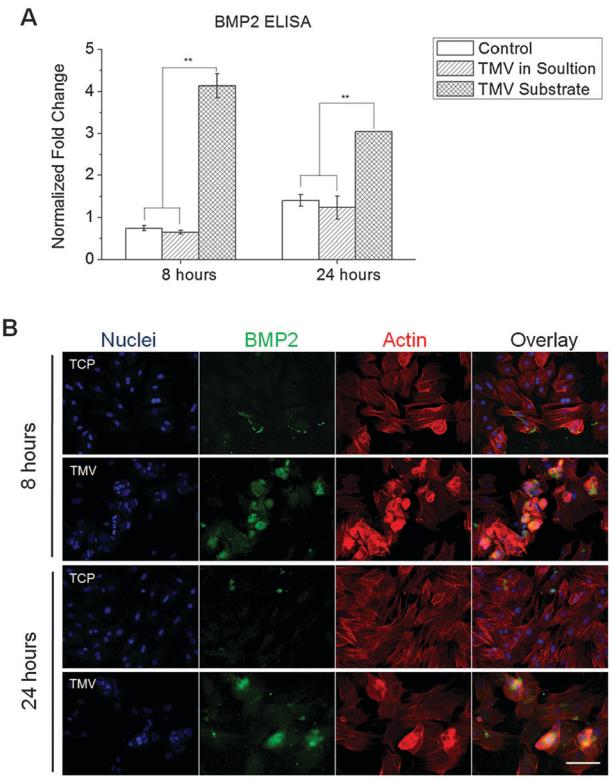

Fig. 3 Differential expression and localization of BMP2 analyzed by ELISA and immunohistochemical staining. (A) Quantification of BMP2 protein expression at 8 and 24 hours normalized to the cell number by ELISA. The values are expressed as fold change compared to cells on TCP before osteoinduction. The error bars denote ±1 s.d. ** $p < 0.05$ based on ANOVA. (B) Cells on TCP control or TMV substrates were collected at 8 and 24 hours after osteogenic induction. At both time points, cells on TMV-coated surfaces expressed more BMP2 protein and the protein is highly expressed at cell aggregates. Color representation: nucleus (blue), BMP2 (green), actin (red). Scale bar is 100 μm.

only TMV coated surfaces induced a significant increase in BMP2 mRNA and protein expression after 8 hours of osteogenic induction.

Immunofluorescence imaging of BMP2 revealed that the morphogen is localized to the cell aggregates. As shown in Fig. 3B, BMSCs on TMV stained positive for BMP2 with higher fluorescence intensity at both time points. BMP2 was observed around the cells that formed nodules or aggregates. It is hypothesized that too strong substrate binding may inhibit osteogenic differentiation.[25] Similar to the previous results, the cells with TMV in solution stained poorly for BMP2 (*data not shown*).

The concentrations of secreted BMP2 in conditioned media from the three culture conditions were measured by sandwich based ELISA. Higher concentration of BMP2 was observed in media with cells on TMV substrates, compared to cells on TCP with and without TMV supplemented in the media. The concentrations ranged between 100 and 200 pg mL^{-1} (*data not shown*), which is consistent with that reported in an ultrasound-induced BMP2 secretion within 24 hours.[26]

Enhanced osteogenesis requires TMV coating on substrates

The enhancement in bone differentiation was also assessed by measuring ALP activity and calcium deposition at day 7, 14, and 21. ALP is an early marker of osteogenesis and its activity mediates matrix mineralization. Although only minor upregulation of *ALPL* mRNA levels was observed by RT-qPCR after 24 hours, ALP enzyme activity assays over the course of 3 weeks showed significant differences at day 7 and 14 (Fig. 4A). Similar to the earlier results, the addition of TMV in solution does not increase ALP activity, and only the cells on TMV coated substrates had significantly higher enzyme activities compared to controls. The enzyme activity at day 21 diminishes to the same level for all samples, suggesting that the observed level may be a basal activity level of ALP during the mineralization stage.

Calcium deposition was determined at day 14 by staining with Alizarin Red S. Small nodules of mineralized calcium were observed for controls and cells supplemented with TMV in solution, whereas the nodules were visibly larger for the cells on TMV-coated substrates (Fig. 4B). UV-Vis absorbance measurements of the extracted dyes indicated that the cells on TMV substrates had double content of calcium compared to controls (Fig. 4C). The addition of TMV solution does not enhance matrix mineralization. These results confirm our hypothesis that TMV provides a topographical cue to enhance osteogenic differentiation, likely by changing the surface roughness. The combined results from RT-qPCR, ELISA and immunostaining clearly indicate that BMP2 expression was significantly induced within 24 hours of induction with a peak expression level at 8 hours. The enhancement requires the virus as a substrate rather than as a solution supplement, suggesting the role of topography or surface roughness in TMV-mediated osteogenesis.

Additive effect on BMP2 gene expression

The osteogenic inducing agents that are routinely used for *in vitro* cultures include β-glycerolphosphate, ascorbic acid, and functions dexamethasone. Individual inducers facilitate difference in the bone differentiation process.[21] To examine

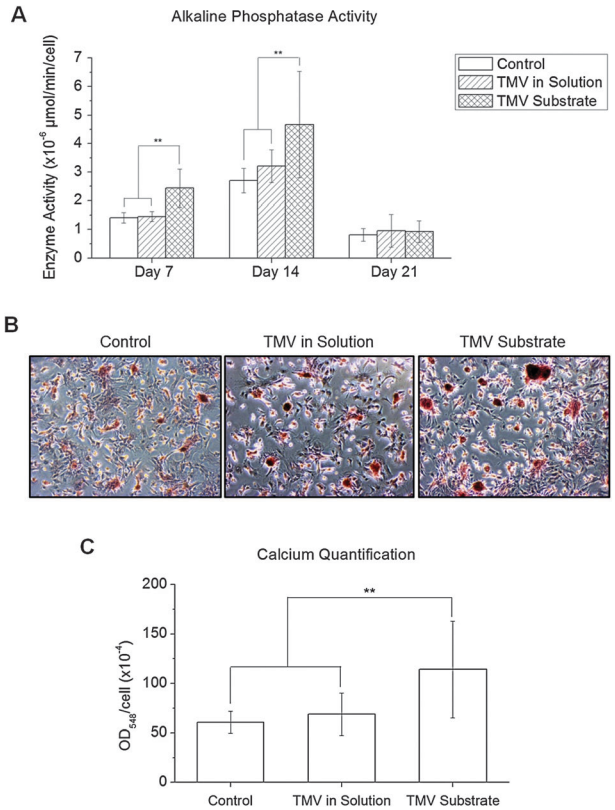

Fig. 4 Cytochemical analysis of the bone differentiation process of BMSCs on TCP, TCP with TMV in media, TMV substrates at 7, 14, and 21 days after osteogenic induction. (A) Alkaline phosphatase activity of cells under three different conditions. Cells on TMV substrates have an increase in enzyme activity at day 7 and 14, whereas the addition of TMV solution does not alter the enzyme activity when compared to control. Alkaline phosphatase activity drops to baseline at day 21 for all conditions. (B) Alizarin red staining of each sample at day 14. (C) Absorbance at 548 nm normalized to the cell number to indicate a relative amount of calcium deposit at day 14 stained by alizarin red solution. The mineralization of cells on TMV substrates doubles that of TCP and TMV in solution, suggesting an improvement in osteogenesis (**$p < 0.05$ based ANOVA). The error bars denote ±s.d.

which osteogenic inducers are required to induce *BMP2* upregulation in BMSCs grown on TMV substrates, the inducers were individually added to different cell cultures and cells were analyzed after 8 hours. Within this time frame, *BMP2* expression levels were the same for cells grown on TCP with or without the three osteogenic inducers (Fig. S2, ESI†). The *BMP2* expression level partially increased for cells grown on TMV coated substrates without any inducers. While the addition of β-glycerolphosphate or L-ascorbic acid 2-phosphate did not upregulate the *BMP2* mRNA level, dexamethasone resulted in a significant increase in the *BMP2* expression level after 8 hours of osteogenic induction (Fig. 5). β-Glycerolphosphate is a phosphate donor for matrix mineralization and in turn increases alkaline phosphatase activity. L-Ascorbic acid 2-phosphate, a stable form of vitamin C, is a source for collagen synthesis which is a major component of bone ECM. However, there is no evidence on the direct effect of these two compounds on modulating BMP2 production. On the other hand, dexamethasone, a glucocorticoid derivative, induced a significant increase in the *BMP2* expression

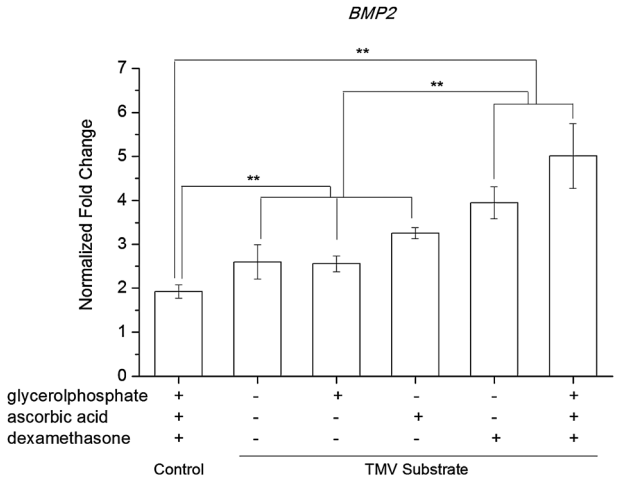

Fig. 5 RT-qPCR analysis of *BMP2* expression in the cells seeded on TCP control and TMV substrates in individual osteogenic inducers for 8 hours. The osteogenic inducers are sodium β-glycerolphosphate, L-ascorbic acid 2-phosphate and dexamethasone. The addition of all three inducing agents resulted in the highest level of BMP2 mRNA. The error bars denote ±s.d. and ** represents $p < 0.05$.

level in BMSCs on TMV substrates. Bi *et al.*[27] illustrated that the treatment of dexamethasone induced BMP2 expression in BMSCs, resulting in a gradual increase of ALP activity over the first 2 weeks. However, the enhanced effect of dexamethasone on BMP2 expression due to surface roughness has not been reported before. This observed enhancement of BMP2 expression from dexamethasone alone is similar to that when all three osteogenic inducers were added to the culture media of cells on TMV wafers (Fig. 5). Although there is a chance that TMV could act as a carrier for dexamethasone internalization, the fact that TMV supplemented media did not enhance BMP2 expression and osteogenesis eliminates this possibility. This clearly highlights the ability of TMV nanosurfaces in the presence of dexamethasone to promote osteogenesis.

To determine if the TMV coating concentrates and immobilizes the chemical inducers to the surface, Quartz Crystal Microbalance with Dissipation (QCM-D) was used to monitor the deposition of each inducer on a TMV-coated substrate. As shown in Fig. S3 (ESI†), there is no significant shift in the resonance frequency of the electrode, which indicates no measurable surface deposition of the osteogenic inducers. While effects of dexamethasone and TMV-coating appear to converge on early BMP2 expression, the initial assessment with QCM-D and the previous TMV solution supplement studies suggest that TMV and dexamethasone do not interact with each other (Fig. S3, ESI†). Furthermore, the virus-coating alone appeared to affect BMP2 expression, which suggests that an alternative regulatory mechanism may be involved.

TMV coating alters cytokine expression

Several other cytokines apart from BMP2 regulate bone remodelling.[28–30] Specifically, inflammatory cytokines from T-cell conditioned media, including TNF-α, IFN-γ, IL-1, IL-17, were shown to induce BMP2 expression.[31] In another study, IL-6, IL-8, monocyte chemotactic protein 1 (MCP-1), macrophage inflammatory protein 1 alpha (MIP-1α), MIP-3α

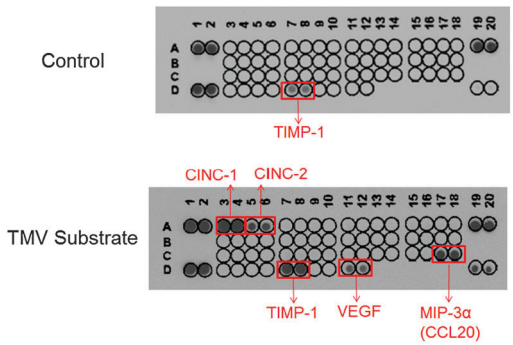

Fig. 6 Comparison of cytokine profiles in culture media of BMSCs on TCP control and TMV substrates for 24 hours, prior to osteoinduction. An antibody array containing 29 different cytokines was used to compare protein profiles produced by cells on different substrates. TIMP-1 was detected in both cultures with higher levels from TMV substrates. However, the productions of some cytokines and growth factors were induced only by TMV-coated wafer, including CINC-1, CINC-2, MIP-3α, and VEGF.

were shown to be involved in fibroblast growth factor-2 (FGF2) mediated osteogenesis.[30] There is also an evidence that the addition of chemokine (C–X–C motif) ligand (CXCL) 12 enhanced BMP2-induced differentiation.[32] We therefore investigated the cells' response to the virus by screening such cytokines or other relevant growth factors which could affect early bone differentiation. Cytokine antibody arrays for 29 cytokines were used to screen the conditioned media from cells cultured on TCP and TMV coated wafers. The media consisting of primary media only was collected after 24 hours of culture and examined. Tissue inhibitor of metalloproteinases-1 (TIMP-1) was the only molecule secreted from both culture conditions, while cytokine-induced neutrophil chemoattractant 1 (CINC-1), CINC-2, MIP-3α, and vascular endothelial growth factor (VEGF) were detected from the conditioned media for the cells on TMV wafers (Fig. 6). According to Kim *et al.*,[30] CINC-1 and MIP-3α recruit neutrophils and monocytes to induce osteogenesis. However, the previous studies did not correlate these cytokines with enhanced BMP2 upregulation during osteogenesis. Future studies on the osteogenic effects of these individual cytokines may reveal their involvement in BMP2-mediated bone differentiation. It could possibly lead to a discovery of new biomaterials to elicit these cytokine productions in order to improve bone healing.

The remaining 24 cytokines, CINC-3, ciliary neurotrophic factor (CNTF), fractalkine, GM-CSF, sICAM-1, IFN-γ, IL-1α, -1β, -1ra, -2, -3, -4, -6, -10, -13, -17, IP-10, lipopolysaccharide induced C–X–C chemokine (LIX), L-selectin, monokine induced by gamma interferon (MIG), MIP-1α, RANTES, thymus chemokine and TNF-α were below the detection limits of the cytokine array.

Actin depolymerization for cells on TMV substrates

Since there was no established direct correlation of other cytokines and osteogenesis, cell morphologies were closely observed prior to osteoinduction. It was demonstrated that BMP2 production was highly localized around the cell nodules (Fig. 3B). Some reports illustrated that culture materials

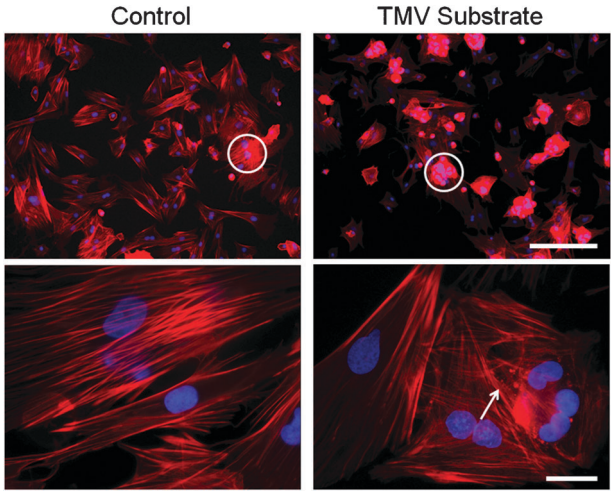

Fig. 7 Cytoskeleton immunochemical staining showing actin polymerization and organization of cells on TCP control and TMV substrates after 24 hours seeding, prior to osteoinduction, at low- (top row) and high-magnification (bottom row). Similar fibrous cytoskeleton organization was observed where cells spread out in both cell cultures. However, in cell aggregates on TMV substrates the actin intensity was higher (white circles) and well-defined actin filament was absent (white arrow). Color representation: nucleus (blue), actin (red). Scale bars are 200 μm for top row and 25 μm for bottom row.

modulate bone differentiation through cytoskeleton organization.[33] The investigation of actin polymerization and organization was carried out to compare cells on TCP and TMV substrates prior to osteoinduction, at which time cell aggregation was first observed. The actin intensity by phalloidin staining was more intense in cells on TMV substrates, indicating higher activity from actin polymerization which could facilitate mobilization of cells to form nodules within 24 hours of cell seeding (Fig. 7). At higher magnification, cells on TCP surfaces maintained highly aligned sarcomeric striations, whereas cells on TMV substrates displayed nonaligned striations. These observations are similar to those obtained from an experiment by Mendonça *et al.*,[25] which demonstrated that cells on a rougher surface topography exhibit an undefined long axis with thicker actin filaments leading to less initial cell spreading followed by enhanced mineralization.

Reduced focal adhesion size

The interaction between cell and ECM is mediated by cell surface receptors (*i.e.* integrins).[34] Vinculins, part of focal adhesion complexes (FACs), couple the integrins to the cytoskeleton allowing crosstalk between ECM and intracellular signalling.[35] Biggs *et al.* highlighted the effects of nanogrooves mediating osteoblastic functions by regulating focal adhesions and subsequent intracellular molecular events.[3] There are other reports showing that integrin-mediated focal adhesion is an important regulator for osteogenesis.[36] Previous studies illustrated that increased localization of vinculin is associated with larger focal adhesion (FA) size and strengthening of adhesion leading to reduced cell motility.[35,37] Smaller size of FAs suggests that BMSCs attached to TMV substrates weakly, whereas larger size of FACs dictates stronger cell–substrate adhesion.[38] While BMSCs on standard TCP exhibited larger

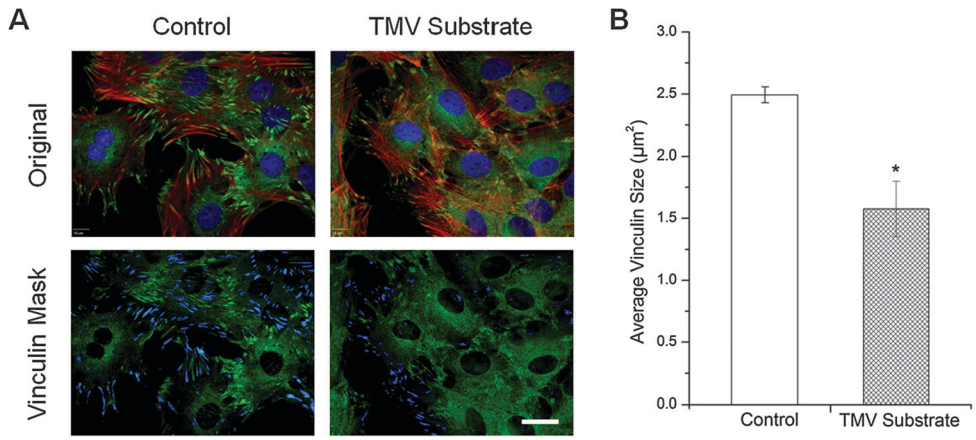

Fig. 8 Immunochemical staining showing the difference in vinculin size of cells on TCP control or TMV substrates for 24 hours. (A) Immunofluorescence images of cells on different substrates for 24 hours prior to osteoinduction (top panel). Color representation: nucleus (blue), vinculin (green), phalloidin (red). The bottom panel illustrates vinculin masking and selection for size analysis. The selected vinculin spots as part of the focal adhesion complex are highlighted in blue. (B) Average vinculin size of cells on either TCP or TMV-coated surface. The error bars denote ±s.d. and $*p < 0.05$ based on equal variance two-tailed Student's *t*-test.

average vinculin size, indicating stronger adhesion to the underlying substrate, the cells on TMV substrates showed smaller FA sizes (Fig. 8A and B). The significantly smaller FA size for cells on TMV substrates is likely to increase cell motility and facilitate the formation of cell aggregates within 24 hours of seeding. Further studies are necessary to establish the correlation of the focal adhesion of BMSCs on virus-coated substrates with the downstream responses.

Experimental

TMV isolation

TMV was isolated and purified according to a protocol previously reported.[8,10]

Preparation of TMV coated substrates

For imaging experiments, 22 × 22 cm glass coverslips (VWR) were cleaned by piranha solution (7 : 3 mixture of 98% H_2SO_4 and 30% H_2O_2) at 75 °C for 2 hours, followed by three washes with water (Millipore Synergy UV system, 18.2 MΩ) and sonication. The dry glass coverslips were immersed in 1% (v/v) of 3-aminopropyltriethoxysilane (APTES) in ethanol for 10 minutes and washed thoroughly with ethanol to remove excess APTES. After drying with nitrogen, APTES coating was crosslinked at 160 °C in a vacuum oven for 1 hour. The wafers were dried and flushed with nitrogen gas for complete drying. For gene expression experiments, APTES coated slides (Lab Scientific Inc.) were cut into 1.5 cm^2 wafers. Both coverslips and slide wafers were sterilized with ethanol before use. For TMV coating, the wafers and coverslips were coated with 0.2 mg mL^{-1} TMV solution diluted in water and the coated substrates were dried overnight in a sterile biosafety cabinet. The virus coverage on the wafers was characterized using tapping-mode AFM images using a NanoScope IIIA MultiMode AFM (Veeco). Si tips with a resonance frequency of approximately 300 kHz, a spring constant of about 40 N m^{-1} and a scan rate of 0.5 Hz were used.

BMSC isolation and expansion

Primary BMSCs were isolated from the bone marrow of young adult 80 g male Wister rats (Harlan Sprague Dawley, Inc.). The procedures were performed in accordance with the guidelines for animal experimentation by the Institutional Animal Care and Use Committee, School of Medicine, University of South Carolina. Cells were maintained in growth medium (DMEM supplemented with 10% fetal bovine serum (FBS), penicillin (100 U mL^{-1}), streptomycin (100 μg mL^{-1}) and amphotericin B (250 ng mL^{-1})) and passaged no more than four times after isolation. To induce osteogenesis, growth media were replaced with osteogenic media consisting of DMEM supplemented with 10% FBS, penicillin (100 U mL^{-1}), streptomycin (100 μg mL^{-1}), amphotericin B (250 ng mL^{-1}), 10 mM sodium β-glycerolphosphate, L-ascorbic acid 2-phosphate (50 μg mL^{-1}) and 10^{-8} M dexamethasone. Media were replenished every 3–4 days.

Quantitative real-time RT-PCR analysis (RT-qPCR)

TMV coated wafers were seeded with 4.5×10^4 cells per wafer and allowed to attach overnight in growth media. The media are replaced with osteogenic media and cultured for 8 and 24 hours. In addition, BMSCs with similar density were seeded on 3.8 cm^2 tissue culture plastic (TCP), with or without TMV in the osteogenic media, for the abovementioned time periods. Furthermore, to determine which osteogenic components are required to enhance osteogenesis on TMV-coated wafers, BMSCs on TMV substrates were cultured in basal media with each osteogenic inducing agent for 8 hours. The cell cultures were terminated at this time point and total RNA was subsequently extracted using an RNeasy mini purification kit, Qiagen. The number of samples for each experiment (n) was two and each experiment was repeated (N) three times.

The quality and quantity of the extracted RNA were analyzed using Bio-Rad Experion (Bio-Rad Laboratories) and were reverse transcribed by using qScript™ cDNA Supermix (Quanta Biosciences). RT-qPCR (iQ5 real-time PCR detection system Bio-Rad Laboratories) was done by the method described

as: 60 cycles of PCR (95 °C for 20 s, 58 °C for 15 s, and 72 °C for 15 s), after initial denaturation step of 5 minutes at 95 °C, by using 12.5 μL of iQ5 SYBR Green I Supermix, 2 pmol μL^{-1} of each forward and reverse primers and 0.5 μL cDNA templates in a final reaction volume of 25 μL. Glyceraldehyde 3-phosphate dehydrogenase (GAPDH) was used as the housekeeping gene. Data collection was enabled at 72 °C in each cycle and C_T (threshold cycle) values were calculated using the iQ5 optical system software version 2.1. The expression levels of differentiated genes and undifferentiated genes were calculated using Pfaffl's method (M. W. Pfaffl, G. W. Horgan and L. Dempfle, Relative expression software tool) for group-wise comparison and statistical analysis of relative expression results in real-time PCR, using GAPDH as the reference gene. Quantification of gene expression was based on the C_T value of each sample which was calculated as the average of three replicate measurements for each sample analyzed. The fold change of each gene expression level is normalized to BMSCs before seeding on different substrates. "Pair Wise Fixed Reallocation Randomization Test" was performed on each sample and a value of $p < 0.05$ was regarded as significant. The primers used for RT-qPCR are shown in Fig. S4 (ESI†). The primers were synthesized commercially (Integrated DNA Technologies, Inc.), and evaluated at an annealing temperature of 58 °C.

Cytochemical staining and quantification

For cytochemical staining, 4.5×10^4 cells were seeded on TMV coated wafers and allowed to attach overnight in basal media. The media were replaced after 24 hours of culture with osteogenic media and cultured for additional 7, 14, and 21 days. As controls, BMSCs were seeded on 3.8 cm^2 TCP at similar densities for the same time periods. CellTiter Blue® assay (Promega) was used to determine the number of cells in each sample one hour prior to cell fixation. The cells were fixed with 4% paraformaldehyde for 15 minutes at room temperature. To determine ALP activity, each fixed sample was incubated in 500 μL of 1-Step *p*-nitrophenyl phosphate solution (Thermo Scientific) for 15 minutes at room temperature. Then the solution was transferred to a new microfuge tube with 250 μL of 2 N NaOH to stop the reaction and the absorbance at 405 nm was measured. The number of samples for each experiment (*n*) was three and each experiment was repeated (*N*) two times.

To compare calcium deposition, fixed samples at day 14 were stained with 0.1% Alizarin red solution (Sigma-Aldrich) pH 4.1–4.5 for 30 minutes. Since the reaction was highly light sensitive, the substrates were wrapped in aluminium foil during the Alizarin red staining. After washing with ultrapure water, 200 μL of 0.1 N NaOH was added to each sample to extract the dye from the sample. The amount of dye was quantified by measuring the absorbance at 548 nm wavelength. Both absorbance values at 405 nm and 548 nm were normalized against the cell number from CellTiter Blue® standard curve. The number of samples for each experiment (*n*) was three and each experiment was repeated (*N*) two times.

Enzyme-linked immunosorbent assay (ELISA)

In order to validate RT-qPCR gene expression at the protein expression level, TMV coated coverslips and uncoated coverslips were seeded with 1.0×10^5 cells per piece. 40 μg of TMV was added to each TMV-in-solution culture. The cultures were terminated at 8 and 24 hours after osteoinduction. CellTiter Blue® (Promega) was used to determine the cell number in each sample one hour prior to cell fixation with 4% paraformaldehyde. Each of the samples was then permeabilized with 0.1% Triton-X 100 for 15 minutes and blocked in 1.5% bovine serum albumin (BSA, Sigma-Aldrich) in PBS for 1 hour at room temperature. After blocking, the cells were incubated overnight with mouse monoclonal antibody targeting BMP2 (R&D systems) at 1 : 100 dilution in blocking buffer. Secondary goat anti-mouse antibody conjugated with horseradish peroxidase (Cayman Chemical) was used at 1 : 1000 dilution for 2 hours at room temperature. After washing, 1 mL of 3,3′,5,5′-tetramethylbenzidine (TMB) solution prepared from TMB ready-to-use tablet (Amresco) was added to each sample, incubating on a rocker for 30 minutes at room temperature. The reaction was stopped by adding 500 μL of 2.0 M H_2SO_4. Absorbance at 450 nm wavelength was measured and then normalized against the cell number. Protein expressions are shown as fold change relative to cells cultured on TCP without osteoinduction. The number of samples for each experiment (*n*) was three and each experiment was repeated (*N*) two times.

Immunofluorescence assays and image analysis

The localization of endogenously expressed BMP2 was examined by immunohistochemical staining. TMV coated coverslips and uncoated coverslips were seeded with 1.0×10^5 cells per piece. The cultures were terminated at 8 and 24 hours after osteoinduction. Cells were fixed in 4% paraformaldehyde at room temperature for 30 minutes. Each of the samples was then permeabilized with 0.1% Triton-X 100 for 15 minutes and blocked in 1.5% bovine serum albumin (BSA, Sigma-Aldrich) in PBS for 1 hour at room temperature. After blocking, the cells were incubated overnight with mouse monoclonal antibody targeting BMP2 (R&D Systems) at 1 : 100 dilution in blocking buffer. Secondary goat anti-mouse antibody conjugated with fluorescein (Chemicon) was used at 1 : 100 dilution for 2 hours at room temperature. Rhodamine–phalloidin (1 : 100 in PBS) was used to stain filamentous actin. Nuclei were stained with DAPI (4,6-diamidino-2-phenylindole, 100 ng mL^{-1}). The samples were then mounted and sealed with clear nail polish before imaging. Images of the stained substrates were taken on an Olympus IX81 fluorescent microscope.

For imaging of actin structure and focal adhesion associated protein, vinculin, uncoated coverslips and TMV coated coverslips were seeded with 1.0×10^5 cells each. Cultures were terminated 24 hours after seeding in basal media. The samples were fixed, permeabilized, and blocked as described above. Cells were incubated with anti-vinculin mouse monoclonal antibody (Neomarkers) at 1 : 200 dilution in blocking buffer. Secondary goat anti-mouse antibody conjugated with fluorescein (Chemicon) was used at 1 : 100 dilutions for 2 hours at room temperature. Rhodamine–phalloidin (1 : 100 in PBS) was used to stain actin. Nuclei were stained with DAPI, and the samples were mounted and sealed with clear nail polish before imaging.

SlideBook™ 5 was used to select and analyze immunofluorescence images of vinculin. After setting the threshold for masks, the criteria used to select vinculin spots to be analyzed were XY shape factor larger than 1.5 and area size between 0.5–15 μm.

The average size of vinculin for each image was calculated, followed by the calculation of average vinculin size of cells on TCP and TMV substrates and the standard deviation from average values of three individual images.

Statistics/data analysis

Data were expressed as mean ± standard deviation (s.d.) of the measured values for cytochemical staining quantification and ELISA. Data were analysed by ANOVA for multiple comparisons, and a *post hoc* test for group to group comparisons, with $p < 0.05$ considered statistically significant.

Cytokine array

Rat Cytokine Antibody Array (R&D Systems) was used according to the manufacturer's instructions. Culture media were collected at 24 hours after cell seeding on TCP control and TMV-coated glass. Briefly, membranes were blocked for 1 hour followed by overnight incubation at 4 °C in 1 mL of cell culture media pre-incubated with provided detection antibody cocktail. After washing, the membranes were incubated with horseradish peroxidase-conjugated streptavidin for 30 minutes. Signals were developed with a Pierce ECL Western Blotting Substrate (Thermo Scientific) and detected on CL-XPosure Film (Thermo Scientific).

Conclusions

Early morphological differences were documented for cells seeded on TMV-coated substrates, wherein the cells often aggregated and spread poorly. The highest BMP2 mRNA and protein levels were detected in cells cultured on TMV-coated substrates after 8 hours of osteoinduction and maintained high *BMP2* mRNA and protein levels even after 24 hours. To eliminate the possibility that the virus may act as a soluble inducer, the virus was supplemented in the media as a solution, however this approach did not afford the same enhancement as the immobilized virus substrate. BMP2 was localized to the cell aggregates, which are only present on cells cultured on TMV coated substrates. Decoupling the three osteogenic agents (dexamethasone, β-glycerophosphate, ascorbic acid) suggests that TMV coating enhances the effect of dexamethasone, but TMV coating alone was sufficient to induce BMP2 gene expression. Screening the media for cytokines revealed the presence of CINC-1, CINC-2, MIP-3α, and VEGF. The surface topography from TMV coating disrupted actin alignment and reduced FA size. The smaller FA indicates a weaker cell–substrate interaction on TMV substrates. The results suggest that a TMV substrate promotes cell aggregation and induces an early onset BMP2 expression.

Although extensive studies with BMP2 show potent osteoinductive effects at early time points, additional studies involving BMP2 knockdown by siRNA and noggin will be necessary to eliminate other possible factors involved in TMV-mediated osteogenesis. Further investigation into other early cell-material and secreted protein–material interactions is necessary for a better understanding of how the TMV coating can promote the endogenous production of BMP2. The regulation of endogenous BMP2 expression will be critical for advanced biomaterial development in bone tissue engineering applications.

Acknowledgements

This work was supported by the US NSF (CHE-0748690), the Alfred P. Sloan Scholarship, the Camille Dreyfus Teacher Scholar Award, and the W. M. Keck Foundation. The authors would like to acknowledge the financial support from State Key Laboratory of Polymer Physics and Chemistry, Changchun Institute of Applied Chemistry, Chinese Academy of Sciences, and National Natural Science Foundation of China (Programs 21128002 and 21104080). Finally, we thank Ms Cheryl Cook for media recipes and Ms Quyen Nguyen for immunohistochemical staining.

References

1 C. E. Ayres, B. S. Jha, S. A. Sell, G. L. Bowlin and D. G. Simpson, *Wiley Interdiscip. Rev.: Nanomed. Nanobiotechnol.*, 2010, **2**, 20–34; D. E. Discher, D. J. Mooney and P. W. Zandstra, *Science*, 2009, **324**, 1673–1677; T. Dvir, B. P. Timko, D. S. Kohane and R. Langer, *Nat. Nanotechnol.*, 2011, **6**, 13–22; R. O. Hynes, *Science*, 2009, **326**, 1216–1219.

2 M. J. P. Biggs, R. G. Richards, S. McFarlane, C. D. W. Wilkinson, R. O. C. Oreffo and M. J. Dalby, *J. R. Soc. Interface*, 2008, **5**, 1231–1242; A. M. Lipski, C. Jaquiery, H. Choi, D. Eberli, M. Stevens, I. Martin, I. W. Chen and V. P. Shastri, *Adv. Mater.*, 2007, **19**, 553–557; C. H. Lohmann, R. Sagun, V. L. Sylvia, D. L. Cochran, D. D. Dean, B. D. Boyan and Z. Schwartz, *J. Biomed. Mater. Res.*, 1999, **47**, 139–151; J. Lovmand, J. Justesen, M. Foss, R. H. Lauridsen, M. Lovmand, C. Modin, F. Besenbacher, F. S. Pedersen and M. Duch, *Biomaterials*, 2009, **30**, 2015–2022; J. Y. Martin, Z. Schwartz, T. W. Hummert, D. M. Schraub, J. Simpson, J. Lankford, D. D. Dean, D. L. Cochran and B. D. Boyan, *J. Biomed. Mater. Res.*, 1995, **29**, 389–401; L. E. McNamara, R. J. McMurray, M. J. P. Biggs, F. Kantawong, R. O. C. Oreffo and M. J. Dalby, *J. Tissue Eng.*, 2010, **1**, 1–13; J. Park, S. Bauer, K. A. Schlegel, F. W. Neukam, K. von der Mark and P. Schmuki, *Small*, 2009, **5**, 666–671; J. Park, S. Bauer, K. von der Mark and P. Schmuki, *Nano Lett.*, 2007, **7**, 1686–1691; Z. Schwartz, J. Y. Martin, D. D. Dean, J. Simpson, D. L. Cochran and B. D. Boyan, *J. Biomed. Mater. Res.*, 1996, **30**, 145–155.

3 M. J. P. Biggs, R. G. Richards, N. Gadegaard, R. J. McMurray, S. Affrossman, C. D. W. Wilkinson, R. O. C. Oreffo and M. J. Dalby, *J. Biomed. Mater. Res., Part A*, 2009, **91**, 195–208.

4 Y. Jiang, B. N. Jahagirdar, R. L. Reinhardt, R. E. Schwartz, C. D. Keene, X. R. Ortiz-Gonzalez, M. Reyes, T. Lenvik, T. Lund, M. Blackstad, J. Du, S. Aldrich, A. Lisberg, W. C. Low, D. A. Largaespada and C. M. Verfaillie, *Nature*, 2002, **418**, 41–49; J. J. Minguell, A. Erices and P. Conget, *Exp. Biol. Med.*, 2001, **226**, 507–520.

5 M. F. Pittenger, A. M. Mackay, S. C. Beck, R. K. Jaiswal, R. Douglas, J. D. Mosca, M. A. Moorman, D. W. Simonetti, S. Craig and D. R. Marshak, *Science*, 1999, **284**, 143–147.

6 Y. L. Si, Y. L. Zhao, H. J. Hao, X. B. Fu and W. D. Han, *Ageing Res. Rev.*, 2011, **10**, 93–103; A. M. Mackay, S. C. Beck, J. M. Murphy, F. P. Barry, C. O. Chichester and M. F. Pittenger, *Tissue Eng.*, 1998, **4**, 415–428; A. C. Drost, S. Weng, G. Feil, J. Schafer, S. Baumann, L. Kanz, K. D. Sievert, A. Stenzl and R. Mohle, *Ann. N. Y. Acad. Sci.*, 2009, **1176**, 135–143; J. Oswald, S. Boxberger, B. Jorgensen, S. Feldmann, G. Ehninger, M. Bornhauser and C. Werner, *Stem Cells*, 2004, **22**, 377–384; Z. Gong, G. Calkins, E. C. Cheng, D. Krause and L. E. Niklason, *Tissue Eng., Part A*, 2009, **15**, 319–330.

7 C. D. Porada and G. Almeida-Porada, *Adv. Drug Delivery Rev.*, 2010, **62**, 1156–1166.

8 G. Kaur, M. T. Valarmathi, J. D. Potts, E. Jabbari, T. Sabo-Attwood and Q. Wang, *Biomaterials*, 2010, **31**, 1732–1741.

9 G. Kaur, M. T. Valarmathi, J. D. Potts and Q. Wang, *Biomaterials*, 2008, **29**, 4074–4081.

10 G. Kaur, C. Wang, J. Sun and Q. Wang, *Biomaterials*, 2010, **31**, 5813–5824.

11 V. Rosen, *Cytokine Growth Factor Rev.*, 2009, **20**, 475–480; O. Ishibashi, M. Ikegame, F. Takizawa, T. Yoshizawa, M. A. Moksed, F. Iizawa, H. Mera, A. Matsuda and H. Kawashima, *J. Cell Physiol.*, 2010, **222**, 465–473; T. Kawasaki, Y. Niki, T. Miyamoto, K. Horiuchi, M. Matsumoto, M. Aizawa and Y. Toyama, *Biomaterials*, 2010, **31**, 1191–1198; J. H. Lee, C. S. Kim, K. H. Choi, U. W. Jung, J. H. Yun, S. H. Choi and K. S. Cho, *Biomaterials*, 2010, **31**, 3512–3519; L. Wang, Y. Huang, K. Pan, X. Jiang and C. Liu, *Ann. Biomed. Eng.*, 2010, **38**, 77–87.

12 Z. S. Ai-Aql, A. S. Alagl, D. T. Graves, L. C. Gerstenfeld and T. A. Einhorn, *J. Dent. Res.*, 2008, **87**, 107–118.

13 H. W. Cheng, W. Jiang, F. M. Phillips, R. C. Haydon, Y. Peng, L. Zhou, H. H. Luu, N. L. An, B. Breyer, P. Vanichakarn, J. P. Szatkowski, J. Y. Park and T. C. He, *J. Bone Jt. Surg., Am. Vol.*, 2003, **85**, 1544–1552.

14 W. McKay, S. Peckham and J. Badura, *Int. Orthop.*, 2007, **31**, 729–734.

15 J. Xu, X. Li, J. B. Lian, D. C. Ayers and J. Song, *J. Orthop. Res.*, 2009, **27**, 1306–1311; T. M. Filion, A. Kutikov and J. Song, *Bioorg. Med. Chem. Lett.*, 2011, **21**, 5067–5070.

16 E. J. Carragee, E. L. Hurwitz and B. K. Weiner, *Spine J.*, 2011, **11**, 471–491; L. B. Shields, G. H. Raque, S. D. Glassman, M. Campbell, T. Vitaz, J. Harpring and C. B. Shields, *Spine J.*, 2006, **31**, 542–547.

17 M. A. Bruckman, G. Kaur, L. A. Lee, F. Xie, J. Sepulvecla, R. Breitenkamp, X. Zhang, M. Joralemon, T. P. Russell, T. Emrick and Q. Wang, *ChemBioChem*, 2008, **9**, 519–523; K. H. Schlick, R. A. Udelhoven, G. C. Strohmeyer and M. J. Cloninger, *Mol. Pharm.*, 2005, **2**, 295–301.

18 L. A. Lee, H. G. Nguyen and Q. Wang, *Org. Biomol. Chem.*, 2011, **9**, 6189–6195; L. Jiang, Q. Li, M. Li, Z. Zhou, L. Wu, J. Fan, Q. Zhang, H. Zhu and Z. Xu, *Vaccine*, 2006, **24**, 109–115; A. A. McCormick, T. A. Corbo, S. Wykoff-Clary, L. V. Nguyen, M. L. Smith, K. E. Palmer and G. P. Pogue, *Vaccine*, 2006, **24**, 6414–6423.

19 Z. Niu, M. A. Bruckman, S. Li, L. A. Lee, B. Lee, S. V. Pingali, P. Thiyagarajan and Q. Wang, *Langmuir*, 2007, **23**, 6719–6724; S. Pennazio and P. Roggero, *Riv. Biol.*, 2000, **93**, 253–281; X. Wang, Z. Niu, S. Li, Q. Wang and X. Li, *J. Biomed. Mater. Res., Part A*, 2008, **87**, 8–14; M. Young, D. Willits, M. Uchida and T. Douglas, *Annu. Rev. Phytopathol.*, 2008, **46**, 361–384.

20 Y. Lin, E. Balizan, L. A. Lee, Z. Niu and Q. Wang, *Angew. Chem., Int. Ed.*, 2010, **49**, 868–872; Y. Lin, Z. Su, G. Xiao, E. Balizan, G. Kaur, Z. Niu and Q. Wang, *Langmuir*, 2011, **27**, 1398–1402.

21 G. Vunjak-Novakovic and R. I. Freshney, in *Culture of Specialized Cells*, ed. R. I. Freshney, Wiley-Liss, Hoboken, New Jersey, 2006.

22 E. Kärner, C.-M. Bäckesjö, J. Cedervall, R. V. Sugars, L. Ährlund-Richter and M. Wendel, *Biochim. Biophys. Acta, Gen. Subj.*, 2009, **1790**, 110–118.

23 L. Wu, L. A. Lee, Z. Niu, S. Ghoshroy and Q. Wang, *Langmuir*, 2011, **27**, 9490–9496.

24 S. Lenhert, M. B. Meier, U. Meyer, L. Chi and H. P. Wiesmann, *Biomaterials*, 2005, **26**, 563–570; A. I. Teixeira, G. A. Abrams, P. J. Bertics, C. J. Murphy and P. F. Nealey, *J. Cell Sci.*, 2003, **116**, 1881–1892.

25 D. B. S. Mendonça, P. A. Miguez, G. Mendonça, M. Yamauchi, F. J. L. Aragão and L. F. Cooper, *Bone*, 2011, **49**, 463–472.

26 C. H. Hou, S. M. Hou and C. H. Tang, *J. Cell. Biochem.*, 2009, **106**, 7–15.

27 L. X. Bi, D. J. Simmons and E. Mainous, *Calcif. Tissue Int.*, 1999, **64**, 63–68.

28 A. Javed, H. Chen and F. Y. Ghori, *Oral Maxillofac. Surg. Clin. North Am.*, 2010, **22**, 283–293.

29 B. a. Cambien, M. Pomeranz, M.-A. Millet, B. Rossi and A. Schmid-Alliana, *Blood*, 2001, **97**, 359–366; C. M. Champagne, J. Takebe, S. Offenbacher and L. F. Cooper, *Bone*, 2002, **30**, 26–31; I. Nakamura, E. Jimi, L. Gerald, in *Vitam Horm*, Academic Press, 2006, vol. 74, pp. 357–370; Z. Q. Xing, C. Y. Lu, D. Hu, Y. Y. Yu, X. D. Wang, C. Colnot, M. Nakamura, Y. L. Wu, T. Miclau and R. S. Marcucio, *Dis. Models & Mech.*, 2010, **3**, 451–458.

30 Y. S. Kim, K. S. Min, D. H. Jeong, J. H. Jang, H. W. Kim and E. C. Kim, *J. Endo.*, 2010, **36**, 1824–1830.

31 L. Rifas, *J. Cell. Biochem.*, 2006, **98**, 706–714.

32 K. Higashino, M. Viggeswarapu, M. Bargouti, H. Liu, L. Titus and S. D. Boden, *Tissue Eng., Part A*, 2011, **17**, 523–530.

33 N. Huebsch, P. R. Arany, A. S. Mao, D. Shvartsman, O. A. Ali, S. A. Bencherif, J. Rivera-Feliciano and D. J. Mooney, *Nat. Mater.*, 2010, **9**, 518–526; A. Mammoto and D. E. Ingber, *Curr. Opin. Cell Biol.*, 2009, **21**, 864–870.

34 B. Geiger, A. Bershadsky, R. Pankov and K. M. Yamada, *Nat. Rev. Mol. Cell Biol.*, 2001, **2**, 793–805.

35 C. Mierke, *Cell Biochem. Biophys.*, 2009, **53**, 115–126.

36 A. J. García and C. D. Reyes, *J. Dent. Res.*, 2005, **84**, 407–413; M. C. Siebers, P. J. ter Brugge, X. F. Walboomers and J. A. Jansen, *Biomaterials*, 2005, **26**, 137–146.

37 L. Peterson and K. Burridge, *Focal adhesions and focal complexes*, University Press, Oxford, UK, 2002.

38 B. Z. Katz, E. Zamir, A. Bershadsky, Z. Kam, K. M. Yamada and B. Geiger, *Mol. Biol. Cell*, 2000, **11**, 1047–1060.

